

# Assessment of modified gold surfaced titanium implants on skeletal fixation

Kasra Zainali,<sup>1</sup> Gorm Danscher,<sup>2</sup> Thomas Jakobsen,<sup>1</sup> Jorgen Baas,<sup>1</sup> Per Møller,<sup>3</sup> Joan E. Bechtold,<sup>4</sup> Kjeld Soballe<sup>1</sup>

<sup>1</sup>Department of Orthopaedics, Orthopaedic Research Center, Aarhus University Hospital, Noerrebrogade 44, Building 1A, DK-8000 Aarhus C, Denmark

<sup>2</sup>Department of Neurobiology, Institute of Anatomy, University of Aarhus, DK-8000 Aarhus C, Denmark

<sup>3</sup>Division of Materials Science and Engineering, Department of Manufacturing and Management, The Technical University of Denmark, DK-2800 Kgs. Lyngby, Denmark

<sup>4</sup>Orthopaedic Biomechanics Laboratory, Midwest Orthopaedic and Minneapolis Medical Research Foundations, Minneapolis, Minnesota, USA

Received 14 February 2012; revised 20 May 2012; accepted 22 May 2012

Published online 30 July 2012 in Wiley Online Library (wileyonlinelibrary.com). DOI: 10.1002/jbm.a.34307

**Abstract:** Noncemented implants are the primary choice for younger patients undergoing total hip replacements. However, the major concern in this group of patients regarding revision is the concern from wear particles, periimplant inflammation, and subsequently aseptic implant loosening. Macrophages have been shown to liberate gold ions through the process termed dissolucytosis. Furthermore, gold ions are known to act in an anti-inflammatory manner by inhibiting cellular NF- $\kappa$ B-DNA binding. The present study investigated whether partial coating of titanium implants could augment early osseointegration and increase mechanical fixation. Cylindrical porous coated Ti-6Al-4V implants partially coated with metallic gold were inserted in the proximal region of the humerus in ten canines and control implants without gold were inserted in contralateral humerus.

Observation time was 4 weeks. Biomechanical push out tests and stereological histomorphometrical analyses showed no statistically significant differences in the two groups. The unchanged parameters are considered an improvement of the coating properties, as a previous complete gold-coated implant showed inferior mechanical fixation and reduced osseointegration compared to control titanium implants in a similar model. Since sufficient early mechanical fixation is achieved with this new coating, it is reasonable to investigate the implant further in long-term studies. © 2012 Wiley Periodicals, Inc. *J Biomed Mater Res Part A*: 101A: 195–202, 2013.

**Key Words:** gold, implant, osseointegration, arthroplasty, experimental

**How to cite this article:** Zainali K, Danscher G, Jakobsen T, Baas J, Møller P, Bechtold JE, Soballe K. 2013. Assessment of modified gold surfaced titanium implants on skeletal fixation. *J Biomed Mater Res Part A* 2013;101A:195–202.

## INTRODUCTION

Noncemented porous coated titanium-alloy implants are the primary choice for younger patients in need of total hip replacements.<sup>1</sup> Although considered a common and successful treatment, up to 20% of the younger hip arthroplasty patients will require revision surgery within 14 years.<sup>2</sup> Revision implants have an even shorter longevity and poorer outcome. It is well accepted that improved early osseointegration and stable mechanical properties are key factors for increasing implant longevity,<sup>3</sup> and therefore technologies such as surface coatings, graft substitutes, and growth factors are intensively investigated.<sup>4–6</sup>

Several experimental studies have proven the immunosuppressive capabilities of gold ions on inflammatory cells. Gold ions inhibit the cellular NF- $\kappa$ B DNA binding activity<sup>7</sup> and reduce I- $\kappa$ B kinase activation<sup>8</sup> and thereby reduce macrophage proliferation, diminish production of proinflammatory cytokines, and inhibit lysosomal enzymes.<sup>9,10</sup> Recent

research have shown that large metallic surfaces release ions when inserted in living tissue that can be found in nearby macrophages.<sup>11</sup> The process, termed dissolucytosis, is defined as extracellular ion liberations and believed to be due to the macrophage's ability to release cyanide ions, alter oxygen tensions, and control the proximity pH.<sup>12</sup> The macrophage's essential role in wound healing and bone repair after orthopedic surgery motivated our investigation of surface coatings that could modulate macrophage function.

The beneficial and important primary inflammatory response after an implant insertion is vital for early osseointegration and mechanical fixation.<sup>13,14</sup> Previously, we compared pure gold coated experimental implants with control titanium-alloy implants in a related press fit implant model and found both a reduction in new bone formation and inferior mechanical stability. These findings were presumably due to an inhibited periimplant remodeling around the press fit implant.<sup>15</sup> The present study introduces a new

**Correspondence to:** K. Zainali; e-mail: kasrazainali@gmail.com

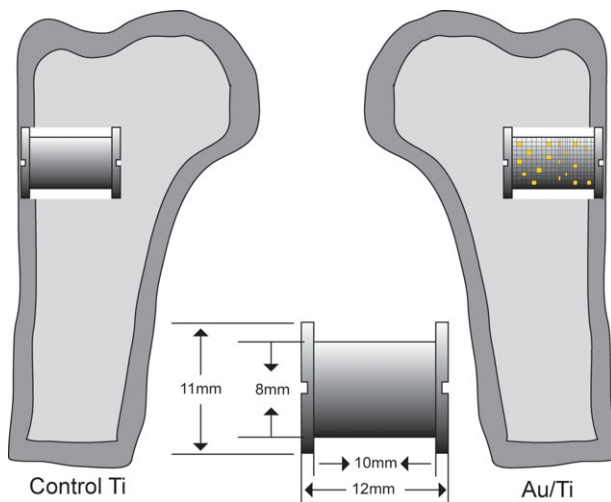


**FIGURE 1.** A schematic overview of the paired implants with specifications inserted in trabecular bone in the proximal part of the humerus. [Color figure can be viewed in the online issue, which is available at [wileyonlinelibrary.com](http://wileyonlinelibrary.com).]

coating that combines gold and titanium as a surface substrate and evaluates it in a gap implant model. The limited address, whether the partial coating influences the implant's early mechanical stability and its bony anchorage, and whether it would decrease fibrous tissue formation. We hypothesized that the new partial gold coating would strengthen mechanical stability and increase osseointegration. Furthermore, we anticipated a reduction of early peri-implant fibrous tissue due to the anti-inflammatory effect. While the anti-inflammatory effect of gold is expected to be most efficacious for modulating a later osteolytic process, we wanted to determine if it also could increase initial fixation by preventing fibrous membrane formation. For this, a gap model was required.

## MATERIALS AND METHODS

### Study design

NIH guidelines for the care and use of laboratory animals were observed, and approval was obtained from our Institutional Animal Care and Use Committee prior initiation of the study. The study was designed as a randomized paired study, and 20 implants were inserted in the proximal region of the humerus bilaterally in ten skeletally mature canines (Fig. 1). The lateral proximal part of the humerus was chosen as implant site, and partial gold-coated implants were inserted in one side and control titanium-alloy implant were inserted in the contra-lateral humerus. The intervention side differed systematically with each animal, with random start.

### Animals

A sample size calculation was made prior to the study. Given standardized conditions, the minimal relevant difference was set to a 50% relative change in the biomechanical fixation. Based upon previous studies, we assumed the standard deviation on the relative change to be 50%. Two-

sided alpha and beta were set to 5 and 20%, respectively. Hence, 10 animals were included per group. The animals were skeletally mature female American Hound dogs. The mean age (SD) was 12.5 months (1.7), and mean weight was 25.1 kg (0.96).

### Implants and gold coating technique

For this study we used 20 custom-made titanium-alloy implants with a plasma-sprayed porous coated Ti-6Al-4V surface. The rough surface coating was kindly applied by Biomet (Warsaw, IN). Each implant was cylindrical with a diameter of 8.0 mm diameter and length of 10 mm. The company determined the mean pore diameter to 480  $\mu\text{m}$ , porosity was 44% and the coating thickness was 1.6 mm. Two 11.0 mm in diameter endplates in each end of the implant created a standardized 1.5-mm gap around each implant.

Half of the porous Ti-6Al-4V surfaces were later coated with a 40–80 nm thin layer of pure gold using the nonreactive physical vapor deposition (PVD) process named magnetron sputtering (Fig. 2). Magnetron sputtering is a magnet field superimposed on a sputtering configuration.<sup>16</sup> The superimposed magnetic field induces an additional force on the charged particles. The force is perpendicular to the speed direction, whereby the charged particles are forced to circulate in a spiral instead of moving in straight lines to the gold target, where the gold for the coating process is placed. The longer pathway increases the number of collisions between mainly electrons and ions and enables the plasma to be self-sustaining at a lower working pressure. The higher collision energy between the target and charged gas ions will apply a higher energy to the sputtered gold

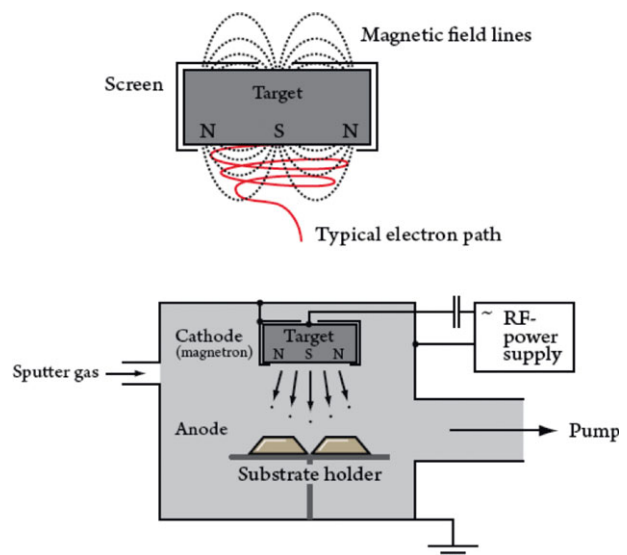


**FIGURE 2.** Typical magnetron configuration with the implant placed in the substrate holder. The sputter gas in this case is Ar. At the cathode a gold plate is placed, and the Au is sputtered with high energy and thereby transferred to the implant surface. The upper figure shows how Ar ions move in a spiral path before dispersing Au ions. [Color figure can be viewed in the online issue, which is available at [wileyonlinelibrary.com](http://wileyonlinelibrary.com).]

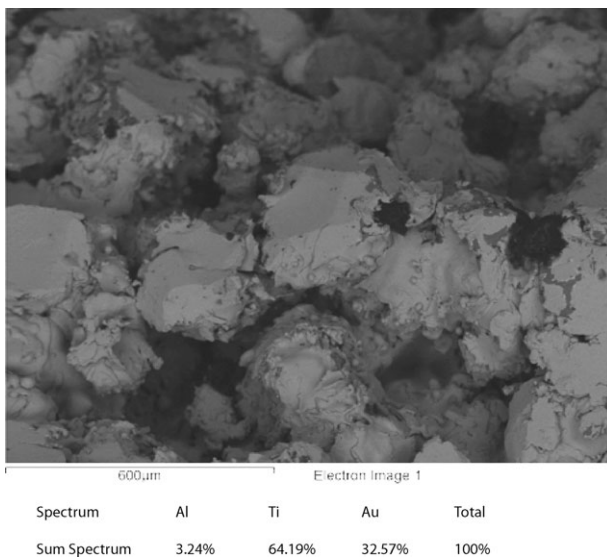


**FIGURE 3.** Scanning electron microscope picture of the porous Ti6Al4V coating after Au coating using magnetron-sputtering process. The thickness of the coating is 40–80 nm.

atoms and improve the adhesion to the porous surface upon the implants.

In this study, the thin gold layer was applied to the porous Ti surface after a sputter cleaning process. The coating procedure is a line-of-sight process, and the porous topology was subsequently not altered (Fig. 3). The bonding mechanisms between gold and titanium are physical and no adhesion promoters such as sputtered Cr were used.

### Surgical procedure

Each procedure was performed under general anesthesia using sterile technique. The proximal part of the humerus was exposed using a lateral extraarticular approach. One Kirschner wire was inserted as a guide wire perpendicular to the surface. An 11 mm cannulated drill was used and drilling was performed slowly to prevent thermal trauma to the bone. The guide wire was removed, the cavity was afterwards cleaned of bone debris and the implant was inserted with its premounted footplate. The cavity was then closed by a topwasher. The operator could not be blinded to which implant was inserted, due to the obvious gold layer. Prophylactic antibiotics were administered preoperatively by administering Rocephin 1 gram IV, and postoperatively Rocephin 1 g IM per day for a minimum of 3 days or until afebrile. Pain relief was administered locally as 2.5 ml Bupivacaine (0.25% 2.5 mg/ml) per incision and systemically 0.01 mg/kg Bupronex (0.3 mg/mL buprenorphine hydrochloride) BID for first and second day postoperatively and SID for the third postoperative day. The dogs were allowed full weight bearing after surgery.

### Specimen preparation

The observation time was 4 weeks. At that time the animals were euthanized and the proximal part of the humerus surrounding the implant was removed, cleaned, and stored at

−20°C. Prior to testing, the bone/implant blocks were thawed. The topwasher was removed and the implant and surrounding bone were cut perpendicular to the long axis of the implant on a water-cooled diamond band saw using an alignment jig (Exakt-Cutting Grinding System, Exakt Apparatebau, Norderstedt, Germany). The bone-implant piece in the proximity of the cortical area (5 mm) was again stored at −20°C and used for biomechanical push-out testing. The remaining bone section was fixed as described below and used for histology.

### Biomechanical testing

Each implant was tested to failure by an axial push-out test performed on a MTS Bionics Test Machine (MTS Systems, Eden Prairie, MN). The specimen was placed central on a metal support jig with a 9.24 mm diameter central gap thereby assuring the recommended distance between implant and jig.<sup>17</sup> The displacement was performed at 5 mm/min with a 5.0-kN load cell. Load and deformation were registered with a computer. For comparability reasons, bone to implant contact area was approximated based on the length and diameter of the implant and used to normalize push-out parameters. Maximal interfacial shear strength ( $\sigma_m$ ) was defined as the first peak of the force-displacement curve ( $F$ ) and was calculated as  $\sigma_m = F/(\pi DL)$ , where  $D$  is the average diameter and  $L$  is the height of the implant. Apparent stiffness was estimated using the maximal slope of the curve and calculated as  $E = (\delta F/(\pi DL))/\delta T$ , where  $T$  is the displacement. Total energy absorption was calculated as the area beneath the curve until implant failure.

### Histological preparation

Tissue blocks were gradually dehydrated in ethanol (70–100%) and embedded in polymethylmethacrylate (PMMA) in a circular jar containing basic fuchsin.<sup>18</sup> Before the sections were made, each implant was randomly rotated along its long axis. This assured uniformly randomized longitudinal sections and thereby optimized the stereological analysis. Sections were cut parallel to the axis with a hard tissue microtome (KDG-95, MeProTech, Heerhugowaard, The Netherlands) around the center part of the implant as described<sup>19</sup> (Fig. 4). Four 30  $\mu$ m sections were cut and counterstained with 2% light green (BDH Laboratory Supplies, Poole, England). This procedure stains bone green and non-mineralized tissue red.

Each remaining bone and implant piece was then re-embedded in PMMA and its gap divided into four different levels with 250  $\mu$ m distance apart. From each level two parallel 7- $\mu$ m sections were cut on a polycut machine and stained with Goldner Trichrome (GT). This stains bone green and osteoid surfaces red.

### Stereological histomorphometrical evaluation

Each implant was analyzed histomorphometrically using a stereological software program (newCAST, Visiopharm A/S, Horsholm, Denmark). The investigator was blinded to the evaluation of the specimens. Fields of vision from a light

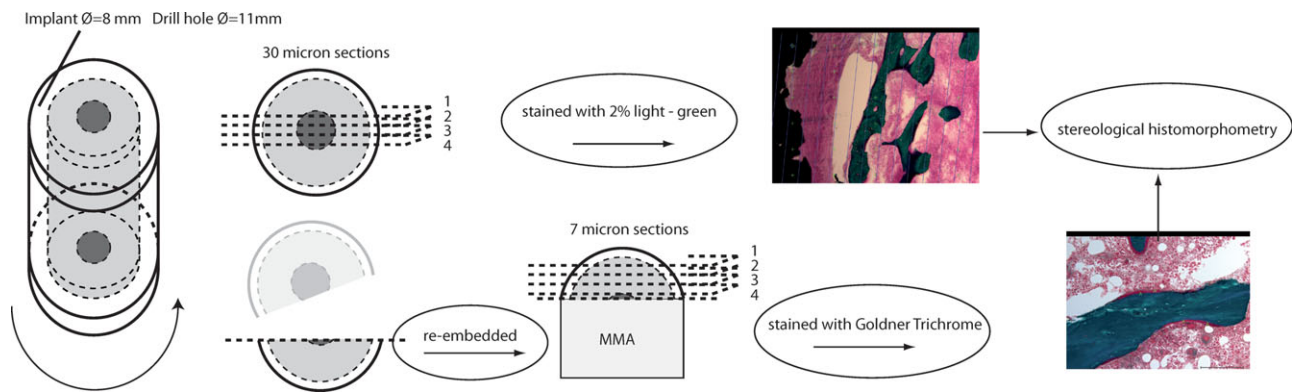


**FIGURE 4.** A schematic overview of specimen preparation leading to histological evaluation: After random orientation around the vertical axis, central sections are cut, before re-embedding of remaining bone piece and sectioning for GT staining. [Color figure can be viewed in the online issue, which is available at [wileyonlinelibrary.com](http://wileyonlinelibrary.com).]

microscope were captured on a computer and a grid was superimposed on the microscopic fields.

The four parallel 30- $\mu$ m sections, stained with basic fuchsin and light green from the centerpiece of the implant, were used. Two well-defined zones were outlined from a median line across the porous implant surface and outward with zone 1 (0–500  $\mu$ m) counting 1177 points (range 886:1464) and with zone 2 (500–1500  $\mu$ m) counting 2150 points (range 1494:2888). Gap healing, also called ingrowth was calculated as volume fractions of new woven bone, fibrous tissue, and marrow space. These were quantified by point-counting technique.<sup>20</sup> Each section was analyzed, and data from all four specimens were accumulated. On the implant surface, the area fractions of the same tissues were quantified by the line-interception technique.<sup>21</sup> Approximately 892 line intersections were counted per implant (range 526:1415). These techniques provide highly reliable results with negligible bias.<sup>22</sup>

The 7- $\mu$ m GT thin sections were used to measure the amount of total bone surface, bone resorption, and bone formation. Linear intercept technique was used to count the bone surface on a user made 2500  $\mu$ m x 4500  $\mu$ m area, and the data were accumulated. Approximately an average of 1793 intersections (range 942:3086) were counted on each specimen. Osteoclast surfaces with bone resorption were recognized as surface areas with resorption lacunae or osteoclasts. Osteoid surfaces were stained red due to the GT preparation. The bone formation was recognized as osteoid surfaces and reabsorptive surfaces were evaluated as osteoclast surfaces or reabsorbed lamellar bone. Osteoclast surfa-

ces and osteoid surfaces were calculated as percentage of total bone surface area.

### Statistics

Data were log-transformed and found normally distributed. Student's paired *t*-test was used to test for differences between treatment groups. Two-tailed *p*-values <0.05 were considered to be statistically significant.

## RESULTS

### Animals

There were no postoperative complications and all canines were fully weight bearing within 2 days after surgery. All animals completed the observation period of four weeks. There were no clinical signs of infection during this period or at termination, and the dogs behaved normally and remained healthy.

### Mechanical results

The biomechanical results are shown in Table I. Mechanical test specimens from one dog were excluded due to a technical error during push-out procedure of its control implant. The push-out tests showed no statistically significant differences between the partial gold-coated surface and the control titanium surface in maximal shear strength, ultimate shear stiffness, or total energy absorption.

### Histomorphometrical results

The paired histomorphometrical data from the 30  $\mu$ m centerpiece sections can be found in Figure 5. There were no

**TABLE I.** Biomechanical results are depicted with absolute mean values for each group. The relative median ratio is shown and the parentheses show 95% CI

	Max Shear Strength (MPa)	Max Shear Stiffness (MPa/mm)	Total Energy Absorption (kJ/m <sup>2</sup> )
AuTi	1.94 (1.30–2.90)	6.29 (4.18–9.48)	452 (302–678)
Ti	1.87 (1.38–2.53)	5.78 (4.33;7.72)	504 (338–752)
AuTi/Ti %	1.04 (0.67–1.60)	1.09 (0.69–1.72)	0.90 (0.55–1.45)
<i>p</i> values	<i>p</i> = 0.85	<i>p</i> = 0.68	<i>p</i> = 0.62



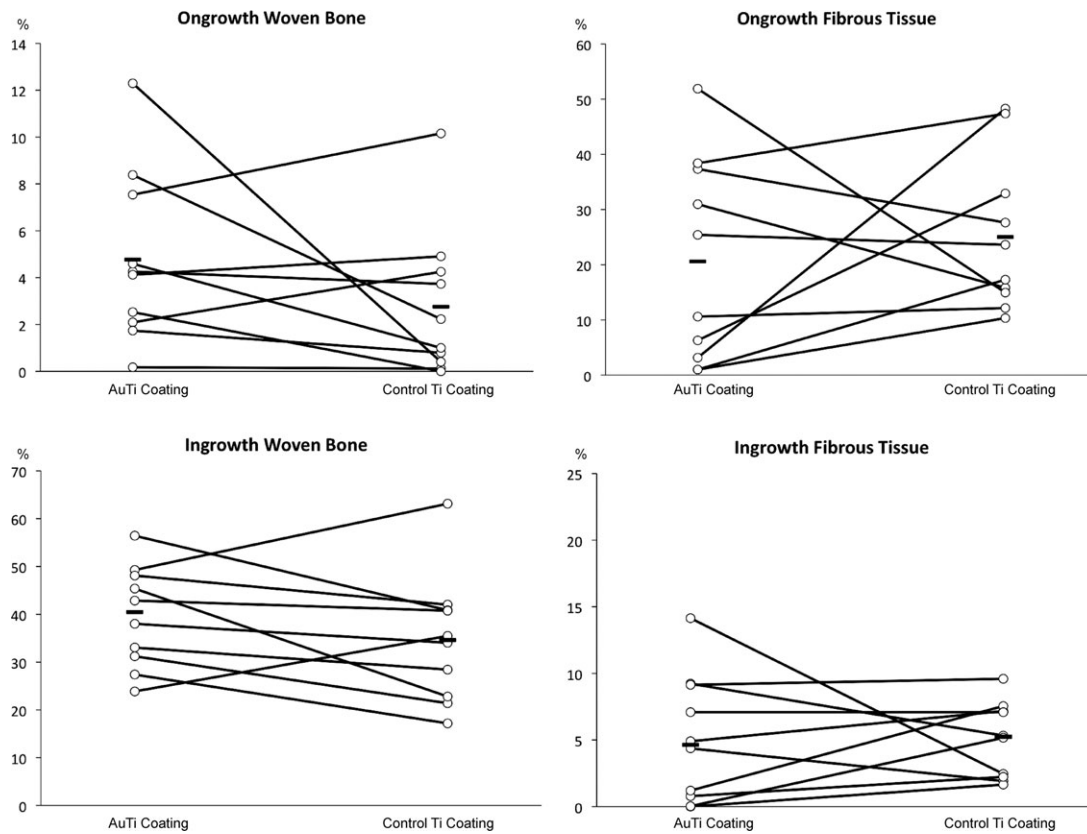


**FIGURE 5.** The histology data is shown in the graphs. Ongrowth is defined as tissue-to-implant contact in percentage of total tissue. Ingrowth is defined as tissue density in the gap in percentage of total tissue. The paired data from each animal is connected with a line. The mean value of each group is also shown with a line in each group. No statistically significant differences were found.

statistically significant differences in bone ongrowth, fibrous ongrowth, periimplant bone volume, and periimplant fibrous volume. At the implant surface, mean bone ongrowth with the partial gold-coated surface was found to be 4.8% compared with 2.8 % bone ongrowth on the titanium-alloy implants ( $p = 0.23$ ). Mean fibrous tissue was 20.6% compared with 25.0% ( $p = 0.14$ ). The mean of total periimplant bone volume increased to 39.6% from 34.6% compared

with titanium alloy implants ( $p = 0.14$ ), whereas mean value for periimplant fibrous tissue was 5.1% in the partial gold-coated group and 5.0% in control group ( $p = 0.25$ ).

Two animals had to be excluded in the 7  $\mu\text{m}$  GT specimen histomorphometrical analysis. This was due to preparation difficulties in one implant in the partial gold-coated group (animal 2) and one in the control group (animal 8). Data from the remaining animals is depicted in Figure 6.

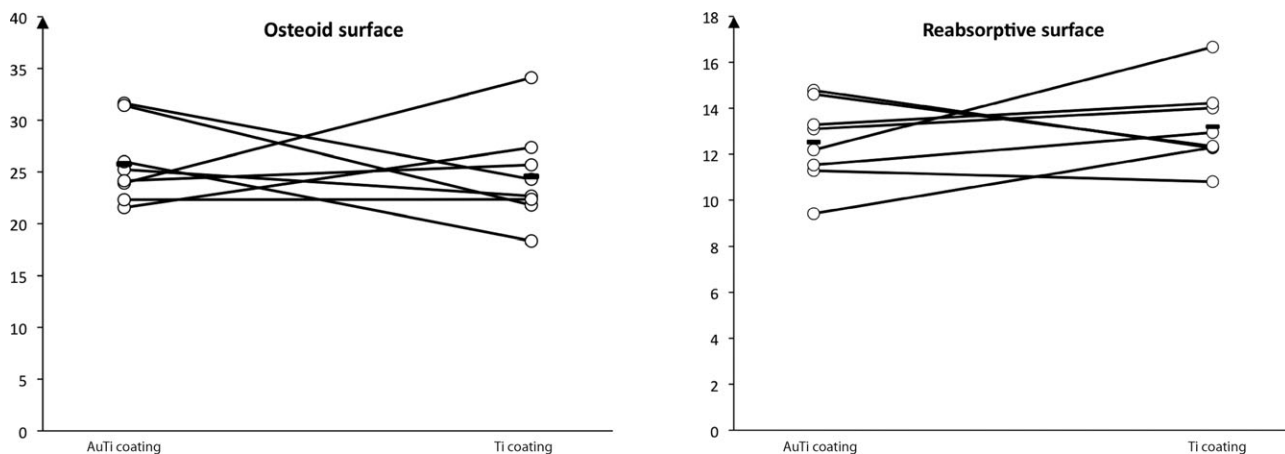


**FIGURE 6.** Bone remodeling shown as osteoid surface and reabsorptive surface of total bone surface in the gap. The paired results are connected by a line for each animal and mean value is also shown. No statistically significant differences were found.

The two groups were similar and no statistically significant differences could be measured.

## DISCUSSION

This study investigated a new gold coating of experimental titanium-alloy implants, referred to as AuTi coating. Biomechanical implant strength, stereological evaluation of implant-to-tissue contact, and periimplant tissue density were used as parameters. Bone-remodeling activity in adjacent tissue was measured. No statistically significant differences could be found in mechanical strength after 4 weeks when compared to control Ti implants. Furthermore, no apparent histological differences could be measured in bone ongrowth, periimplant bone ingrowth or fibrous tissue formation. Finally, the bone remodeling activity in the periimplant gap remained unaltered. The new AuTi coating showed interesting results when compared with previous gold-coated implants, as mechanical and histological parameters were not negatively influenced as seen earlier.

Canines were used as experimental animals because of their human-like bone structure and bone density.<sup>23</sup> The proximal part of the humerus was chosen as implant site because of its rich amount of trabecular bone. The study was designed to imitate the cancellous region of a cementless joint replacement, and the implant was inserted in the center of the cavity surrounded with an empty gap. This model is highly standardized and reproducible. The empty gap-model was used to allow inflammation and fibrous tissue early in the process, since we wished to investigate whether metallic gold also could reduce an inflammatory response in bones. Furthermore, the design allowed quantification of the amount of bone and fibrous tissue in contact with the implant and also thorough analysis of the periimplant tissue. Contralateral implants allowed a paired study design that makes comparison of AuTi implants and control Ti implants within each animal possible. The biological difference between the animals, which is quite large, was thereby controlled for. This allowed a significant reduction in the number of canines needed in the study. The model is well established and has resulted in numerous publications, since it is standardized and reproducible. However, the model is limited, as the unloaded implant model does not consider any effect of weight-bearing conditions to the implants. Furthermore the implants were inserted using a transcortical method, which does not concur with clinical procedures such as total joint replacements. These do not benefit from the healing of the periosteum. Although all data was paired and results were compared within the same animal, clinical perspectives should bear these limitations in mind.

This study compared two different implant surface coatings. The implant surface topologies are considered comparable since the gold coating, which is applied on titanium-alloy, is only 40–80 nm thick. The gold surface is applied with a “line-of-sight” method where gold does not cover the deep pore structures and the percentage of gold surface is therefore relatively low. The integrity of the coating was not tested prior insertion. However, a careful implant insertion was allowed with the use of the empty gap model and

therefore no stress was applied to the implant during the insertion. Observation time of four weeks was used in this study, as previous studies have been able to show relevant differences within four weeks with the same model.<sup>6</sup> With the same four week observation time, a significant difference was found in our former study with the comparison of complete gold-coated implants with control titanium-alloy implants (reduced fixation with press-fit implant with full gold coating).<sup>15</sup> Of note, a longer observation time may result in a measurable difference but may also show a general increase in new bone on both surfaces. The results should also be considered with care, since one animal was lost in the mechanical results and two were lost in the histology results. No statistically significant differences were found, and with the decrease in study strength, the risk of type 2 error should be considered.

We hypothesized that the intermittent AuTi coating would prevent the negative effects of a full gold coating (previously reported) and increase short-term mechanical strength and osseointegration compared to a titanium-alloy implant. Mechanical parameters showed slight increase in maximal shear strength and maximal shear stiffness, although these results were not statistically significant. Additionally, histological analysis of the periimplant gap healing showed a slight increase in bone ongrowth and bone ingrowth in the AuTi group. These results were again not statistically significant. Overall we were not able to find any difference in the early osseointegration of the two surface coatings. However, the results were encouraging, since the AuTi coating was an improvement compared to the previous pure gold coating. In that study, the total gold surface coating resulted in 35% reduction in bone ongrowth and 40% decrease of mechanical strength after 4 weeks. This was primarily reasoned to be due to gold’s anti-inflammatory capabilities, and not any direct inhibition of osteoblasts.

This reduced bone mineralization corresponds with the work of Thomsen et al. who found reduced bone formation on gold-coated screws.<sup>24</sup> This was however in cortical bone, whereas in this study implants were inserted into trabecular bone. Thomsen et al. considered gold as a noble metal that does not create surface oxides, and thus does not affect the surrounding tissue, whilst titanium surfaces were active oxidized surfaces. Although metallic gold is not active, we reckon that it interacts with the surrounding tissue due to the organism’s always-active inflammatory cells, such as macrophages, and their dissolucytosis of implant surfaces, as illustrated by Danscher<sup>11</sup> and the previous pure gold study.<sup>15</sup> However, gold’s effect is not on cell growth or cell differentiation, and the reduced bone formation is not considered to be due to any toxicity or biocompatibility issues. Furthermore Cortizo et al. showed no significant differences in proliferation or cell survival, when osteoblast-like cells were subjected to titanium or gold.<sup>25</sup> The AuTi surface had a reduced amount of gold surface area. The differences in bone mineralization between these studies could be explained due to a dosage-dependent mechanism related to the inflammatory response described later. Since the early

bony anchorage is predictive of the implant's longevity,<sup>3,26</sup> an adequate sufficient fixation was necessary, before long-term investigations were performed. We therefore suggest that since the new partial AuTi coating did not differ in immediate early osseointegrative properties compared to titanium-alloy implants and since gold's long-term perspectives may be relevant in reducing later osteolysis, that this should be subject to further study.

The anti-inflammatory capabilities of gold ions are well established although the underlying mechanisms are not all fully understood. Gold ions are capable to inhibit macrophages and inhibit lysosomal enzymes in phagocytotic cells, once they are intracellular.<sup>9,10,27</sup> Their ability to suppress NF- $\kappa$ B-binding activity<sup>7</sup> and reduce I- $\kappa$ B-kinase activation<sup>8</sup> result in reduction in proinflammatory cytokines. The important findings that gold is not an inert metal, but slowly dissolves in the organism by the process termed dissolution, makes it possible to use metallic gold to establish a safe local "gold cure".<sup>28</sup> Recently, Pedersen et al. showed that large size metallic gold particles, unable to be phagocytosed, inserted in the mouse brain reduces TNF-alpha levels, oxidative DNA damage and the amount of microglia cells.<sup>29</sup> Hence the local inflammatory response was significantly reduced. Our empty gap model allowed a visible postoperative inflammatory response with fibrous tissue surrounding the implant. We hypothesized that the introduced AuTi surface released gold ions and that they would reduce the inflammatory process and subsequently minimize the fibrous ongrowth and periimplant fibrous tissue. This was not observed, although gold ions were supposed to inhibit fibroblasts. While gold ion release and uptake in macrophages was not imaged in the present study, we assume it was likely to have happened, as several publications confirm findings of intracellular gold ions next to a metallic gold implant.<sup>11,12</sup> Based on our studies with implants and varying gap sizes, it is possible that the 1.5-mm gap allowed an extensive early inflammation, which the AuTi coating was not capable to subdue.

We know from the clinic that implants not inserted sufficiently stable in bone have a tendency to become encapsulated in fibrous tissue.<sup>30</sup> On the other hand, implants inserted press fit with a proper osseointegration can later be found encapsulated in fibrous tissue due to particle-induced macrophage activation, periimplant inflammation and secondary osteolysis. These two inflammatory processes are quite different. The first response is caused partly by the lesion itself and partly as a foreign body reaction towards the implant.<sup>31,32</sup> The fibrous tissue is produced because there is space for fluid accumulation, and connective tissue is the quickest tissue to fill the gap. The immediate postoperative inflammatory response has already been shown as a vital part of implant osseointegration and fracture healing.<sup>13</sup> However, the later response could be an activation of a cascade-like sequence, where macrophages were activated due to particle debris that may be accumulating.<sup>33</sup> Particle-induced macrophage activation and the role of NF- $\kappa$ B in osteoclastogenesis and osteolysis is well documented.<sup>34</sup> Gold's capability to inhibit NF- $\kappa$ B-binding activity and the

possibility to suppress this process locally with the use of metallic gold on the implant surface is interesting. The fibrous formation in this study is considered as the first initial response that is too extensive to inhibit by the use of AuTi coating.

Although a difference between the new combined AuTi coating and the titanium coating cannot be dismissed, this study suggests that the osseointegrative properties and the early biomechanical fixation seem to be the same for the two coatings. A further testing of the surface coating in a more clinically relevant model, such as the press-fit model, can elaborate on the immediate osseointegrative properties. Furthermore, a long-term study with particle-induced up-regulation of the local inflammatory response is necessary to highlight the anticipated anti-inflammatory effects of the coating. In summary, the combination of gold with the osseointegrative titanium surface seems reasonable. However, the so-called anti-inflammatory part of the surface (the gold coating) did not significantly influence the initial first inflammatory response, which is deemed beneficial. Hence, its desired late inhibitory effect on any periimplant osteolysis that may come in the long term needs further investigation.

## CONCLUSIONS

This study reveals no statistically significant differences in early mechanical strength, in implant osseointegration, in periimplant bone density, and in bone remodeling activity after the use of our novel AuTi coating on experimental porous implants. This is an improvement since previous pure gold coating showed negative results in a similar model. The extensive documentation of gold's anti-inflammatory effect suggests that this new combined partial gold coating should be further investigated in a long-term and particle-challenged setting, to see if it can reduce particle-induced macrophage activation, and thereby suppress aseptic implant loosening.

## ACKNOWLEDGMENTS

The authors wish to thank Anette Milton, Jane Pauli, Anette Baatrup and Lisa Feng, Orthopaedic Research Laboratory, Aarhus University Hospital for their valuable technical expertise in specimen preparations and guidance. Biomet Inc., USA kindly provided all base elements. All magnetron sputter coating of the AuTi implants was performed at The Technical University of Denmark (DTU), Denmark.

## REFERENCES

1. Heisel C, Silva M, Schmalzried TP. Bearing surface options for total hip replacement in young patients. *Instr Course Lect* 2004; 53:49–65.
2. Overgaard S, Repten J, Vinther MU, Nielsen PT, Varmarken J, Pedersen AB, Bartels P, Solgaard S. *Danish Hip Register Annual Report* 2009. 2010.
3. Karrholm JF, Herberts P, Herberts PF, Hultmark P, Hultmark PF, Malchau H, Malchau HF, Nivbrant B, Nivbrant BF, Thanner J, Thanner J. Radiostereometry of hip prostheses. Review of methodology and clinical results 1997;344:94–110.
4. Jakobsen T, Kold S, Bechtold JE, Elmengaard B, Soballe K. Effect of topical alendronate treatment on fixation of implants inserted with bone compaction. *Clin Orthop Relat Res* 2006;444:229–234.

5. Elmengaard B, Bechtold JE, Soballe K. In vivo study of the effect of RGD treatment on bone ongrowth on press-fit titanium alloy implants. *Biomaterials* 2005;26:3521–3526.
6. Soballe K, Mouzin OR, Kidder LA, Overgaard S, Bechtold JE. The effects of hydroxyapatite coating and bone allograft on fixation of loaded experimental primary and revision implants. *Acta Orthopaedica Scandinavica* 2003;74:239–247.
7. Yang JP, Merin JP, Nakano T, Kato T, Kitade Y, Okamoto T. Inhibition of the DNA-binding activity of NF-kappa B by gold compounds in vitro. *FEBS Lett* 1995;361:89–96.
8. Jeon KI, Jeong JY, Jue DM. Thiol-reactive metal compounds inhibit NF-kappa B activation by blocking I kappa B kinase. *J Immunol* 2000;164:5981–5989.
9. Yanni G, Nabil M, Farahat MR, Poston RN, Panayi GS. Intramuscular gold decreases cytokine expression and macrophage numbers in the rheumatoid synovial membrane. *Ann Rheum Dis* 1994;53:315–322.
10. Persellin RH, Ziff M. The effect of gold salt on lysosomal enzymes of the peritoneal macrophage. *Arthritis Rheum* 1966;9:57–65.
11. Danscher G. In vivo liberation of gold ions from gold implants. Autometallographic tracing of gold in cells adjacent to metallic gold. *Histochem Cell Biol* 2002;117:447–452.
12. Larsen A, Stoltenberg M, Danscher G. In vitro liberation of charged gold atoms: Autometallographic tracing of gold ions released by macrophages grown on metallic gold surfaces. *Histochem Cell Biol* 2007;128:1–6.
13. Gerstenfeld LC, Thiede M, Seibert K, Mielke C, Phippard D, Svarg B, Cullinane D, Einhorn TA. Differential inhibition of fracture healing by non-selective and cyclooxygenase-2 selective non-steroidal anti-inflammatory drugs. *J Orthop Res* 2003;21:670–675.
14. Champagne CM, Takebe J, Offenbacher S, Cooper LF. Macrophage cell lines produce osteoinductive signals that include bone morphogenetic protein-2. *Bone* 2002;30:26–31.
15. Zainali K, Danscher G, Jakobsen T, Jakobsen SS, Baas J, Moller P, Bechtold JE, Soballe K. Effects of gold coating on experimental implant fixation. *J Biomed Mater Res A* 2009;88:274–280.
16. Mattox DH. *Handbook of Physical Vapor Deposition (PVD) Processing: Film Formation, Adhesion, Surface Preparation and Contamination Control*: Noyes Publications; William Andrew, 1998. 948 p.
17. Harrigan TP, Kareh J, Harris WH. The influence of support conditions in the loading fixture on failure mechanisms in the push-out test: A finite element study. *J Orthop Res* 1990;8:678–684.
18. Gotfredsen K, Budtz-Jorgensen E, Jensen LN. A method for preparing and staining histological sections containing titanium implants for light microscopy. *Stain Technol* 1989;64:121–127.
19. Overgaard S, Soballe K, Jorgen H, Gundersen G. Efficiency of systematic sampling in histomorphometric bone research illustrated by hydroxyapatite-coated implants: Optimizing the stereological vertical-section design. *J Orthop Res* 2000;18:313–321.
20. Gundersen HJ, Bendtsen TF, Korbo L, Marcussen N, Moller A, Nielsen K, Nyengaard JR, Pakkenberg B, Sorensen FB, Vesterby A. Some new, simple and efficient stereological methods and their use in pathological research and diagnosis. *APMIS* 1988;96:379–394.
21. Baddeley AJ, Gundersen HJ, Cruz-Orive LM. Estimation of surface area from vertical sections. *J Microsc* 1986;142(Part 3):259–276.
22. Baas J. *Adjuvant Therapies of Bone Graft Around Non-Cemented Experimental Orthopedic Implants Stereological Methods and Experiments in Dogs [Supplement]*. Aarhus: Aarhus University; 2008. p1–43.
23. Aerssens J, Boonen S, Lowet G, Dequeker J. Interspecies differences in bone composition, density, and quality: Potential implications for in vivo bone research. *Endocrinology* 1998;139:663–670.
24. Thomsen P, Larsson C, Ericson LE, Sennerby L, Lausmaa J, Kasemo B. Structure of the interface between rabbit cortical bone and implants of gold, zirconium and titanium. *J Mater Sci Mater Med* 1997;8:653–665.
25. Cortizo MC, De Mele MF, Cortizo AM. Metallic dental material biocompatibility in osteoblastlike cells: Correlation with metal ion release. *Biol Trace Elem Res* 2004;100:151–168.
26. Ryd L, Albrektsson BE, Carlsson L, Dansgard F, Herberts P, Lindstrand A, Regner L, Toksvig-Larsen S. Roentgen stereophotogrammetric analysis as a predictor of mechanical loosening of knee prostheses. *J Bone Joint Surg Br* 1995;77:377–383.
27. Vernon-Roberts B. Action of gold salts on the inflammatory response and inflammatory cell function. *J Rheumatol Suppl* 1979;5:120–129.
28. Danscher G, Larsen A. Effects of dissolucytotic gold ions on recovering brain lesions. *Histochem Cell Biol* 2010;133:367–373.
29. Pedersen MO, Larsen A, Pedersen DS, Stoltenberg M, Penkowa M. Metallic gold reduces TNFalpha expression, oxidative DNA damage and pro-apoptotic signals after experimental brain injury. *Brain Res* 2009;1271:103–113.
30. Bauer TW, Schils J. The pathology of total joint arthroplasty. I. Mechanisms of implant fixation. *Skeletal Radiol* 1999;28:423–432.
31. Futami T, Fujii N, Ohnishi H, Taguchi N, Kusakari H, Ohshima H, Maeda T. Tissue response to titanium implants in the rat maxilla: Ultrastructural and histochemical observations of the bone-titanium interface. *J Periodontol* 2000;71:287–298.
32. Kienapfel H, Sprey C, Wilke A, Griss P. Implant fixation by bone ingrowth. *J Arthroplasty* 1999;14:355–368.
33. Ingham E, Fisher J. The role of macrophages in osteolysis of total joint replacement. *Biomaterials* 2005;26:1271–1286.
34. Abu-Amer Y, Darwech I, Otero J. Role of the NF-kappaB axis in immune modulation of osteoclasts and bone loss. *Autoimmunity* 2008;41:204–211.